

CuInS₂ grown under elevated pressures, Part 2: Optical defect characterization

N. Dietz, M.L. Fearheiley and H.J. Lewerenz

Hahn-Meitner-Institut, Bereich Photochemische Energieumwandlung
Glienicke Str. 100, Postfach 39 01 28, 1000 Berlin 39

Abstract

We present information obtained by a new angle resolved reflection spectroscopy on the defects in CuInS₂ single crystals. The method permits the room temperature detection of small variations of the complex dielectric function ϵ . The variation of $\epsilon = \epsilon_1 - i\epsilon_2$ is correlated to the defect centers and their energetic position in the band gap. The defect levels determined from this method are compared to photoluminescence and transmission spectroscopy results.

1. INTRODUCTION

The analysis of electronic defects is of crucial importance for semiconductor material development. To satisfy the requirement of defect characterization in electronic devices and their components, a series of optical detection methods were developed. These methods, for example photoluminescence (PL) [1-7], electroreflectance (ER)[8, 9], photorelectance[1, 10] standard reflectivity[1, 11] and absorption measurements[12] are limited in sensitivity or applicability. To develop new materials for solar applications different methods are necessary to tailor its production conditions. Therefore we have developed an experimental method based on the measurement of the Brewster angle (also called pseudo-Brewster angle[13] or first Brewster angle[14]) ϕ_B and the reflectivity R_p for light polarized parallel to the plane of incidence. The method allows accurate determination of the optical constants ϵ_1 and ϵ_2 as well as small variations in the optical constants, which result from defects whose energy levels lie within the band gap.

2. EXPERIMENTAL

The optical constants were obtained by Brewster angle spectroscopy (BAS)[15, 16] in an energy range from 0.7 eV to 1.8 eV. The schematic diagram of the experimental set-up is shown in Fig. 1. A tungsten iodine lamp was used as light source in combination with a Kratos monochromator. The monochromatic beam is split into a reference and a signal beam. The signal beam is polarized parallel to the plane of incidence using a Glan-Thompson polarizer, P. The polarized light is

focused onto a mirror-type specularly reflecting sample which is held at an angle, ϕ , close to the Brewster angle, ϕ_B . The reflected intensity is detected by a cooled Si- (0.4 - 1 μm) or Ge-detector (0.8 - 1.7 μm). For analysis of the reflected intensity and the Brewster angle position, the signal beam was measured as a function of the angle ϕ . The minimum was determined by a least squares fit and the reflectivity R_p was determined by comparison with the reference beam. A standard lock-in technique was used for data acquisition.

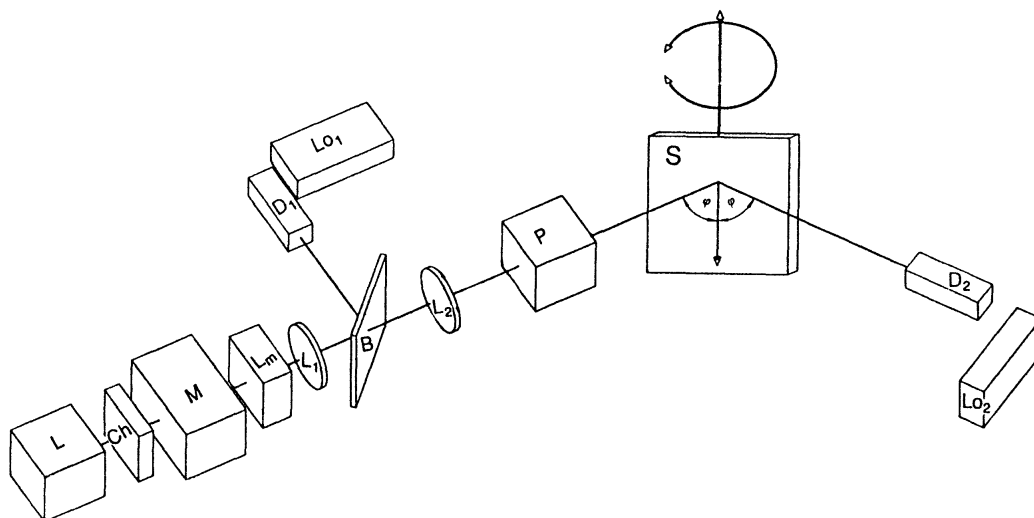


Figure 1 Schematic diagram of the experimental set-up: L: Lamp; Ch: Chopper; M: Monochromator; L_m : achromatic lens system; L_1, L_2 : Slits; B: Beamsplitter; P: Polarizer; D_1, D_2 : detectors; Lo_1, Lo_2 : Preamplifier; S: Sample

Photoluminescence (PL) measurements were performed by using an Eximer-Laser (EMG 53 MSC-Lambda Physics) to pump a Dye-Laser (FL 2001-Lambda Physics). The excitation energy was 2.3 eV, the beam power 18 mW. The samples were mounted into a TIC 303M (Cryovac) continuous flow liquid helium cryostat. The emission spectra were recorded using a Spex 1401 monochromator and photomultiplier (RCA 7071).

Transmission measurements were done with an Omega spectrophotometer (Bruin Instruments) using the two-beam reference method in an energy range from 0.70 eV up to 4 eV.

3. RESULTS AND DISCUSSION

3.1 GaAs:

To test the sensitivity as well as the accuracy of the BAS method, the defect structures of GaAs, which were already reported[17-20], were investigated.

Fig. 2a shows the spectral dependence of the Brewster angle ϕ_B and the reflectivity R_p at ϕ_B for n-GaAs(100) with carrier concentration smaller than 10^{16} cm^{-3} . Below

the bandgap at $E_0=1.42$ eV the well known intrinsic electron traps at 0.78 eV (L_{12}), 0.83 eV (L_2) and the reported absorption centers at 0.95 eV, 1.10 eV and 1.30 eV [19] are clearly revealed.

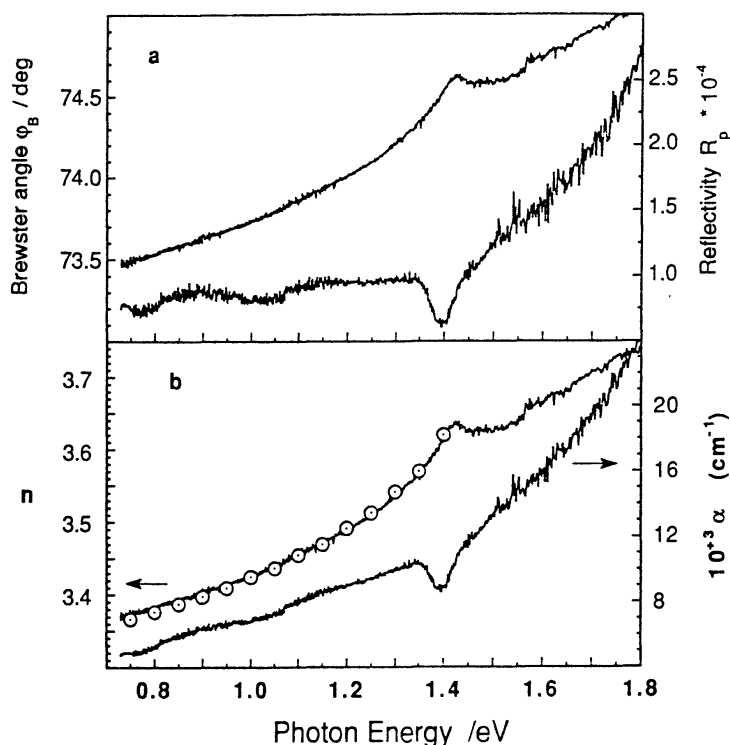


Figure 2: a) Measured spectral dependence of the Brewster angle, ϕ_B , and the reflectivity, R_p , at ϕ_B for undoped GaAs (100). b) Refractive index n {compared with literature values[21] (open circles)} and absorption coefficient α , calculated using the analytical BAS method[16].

The calculated refractive index n (fig. 2b) compared with data obtained by the prism-diffraction method[21] (open circles) show excellent agreement with an error of $\pm 0.1\%$. Near the band gap, the absorption coefficient α agrees well with literature values [22, 23]. Below the band gap lower values for the absorption coefficient are reported[24-26].

3.2 CuInS₂:

Three different types of CuInS₂ samples were investigated. All samples were grown with the gradient freeze technique[27] using Argon overpressure. By variation of the grown condition [28] crystals, which varied from semi-insulating (Type A: resistance $\rho \approx 7500 \Omega \text{ cm}$; mobility $\mu \approx 24 \text{ cm}^2 / \text{V s}$; carrier concentration $cc=4.2 \cdot 10^{15} \text{ cm}^{-3}$), moderately p-type (Type B: resistance $\rho \approx 250 \Omega \text{ cm}$; mobility $\mu \approx 45 \text{ cm}^2 / \text{V s}$; carrier concentration $cc=6.5 \cdot 10^{14} \text{ cm}^{-3}$) to lamellarly structured material occurs. The experimental results for the lamellar structure material will be published elsewhere[29].

For the ternary chalcopyrite CuInS_2 , the optical properties near the band gap ($E_g = 1.55 \text{ eV}$) have been studied using measurements of absorption[1, 12, 30], reflectivity[1] electroreflectance and photoreflectance[1, 10]. The defect structures were mostly investigated by photoluminescence measurements[2-5, 7]. The optical defect characterization as a supplement to the usually complex electronic characterization has not yet been performed. To do this, BAS provides a simple and fast method. The sensitivity of this method is shown in Fig. 3 on a reflectivity plot at various angles of incidence φ for CuInS_2 (Type A). For an incidence angle $\varphi=30^\circ$ a broad reflection structure below the band gap at 1.30 eV occurs.

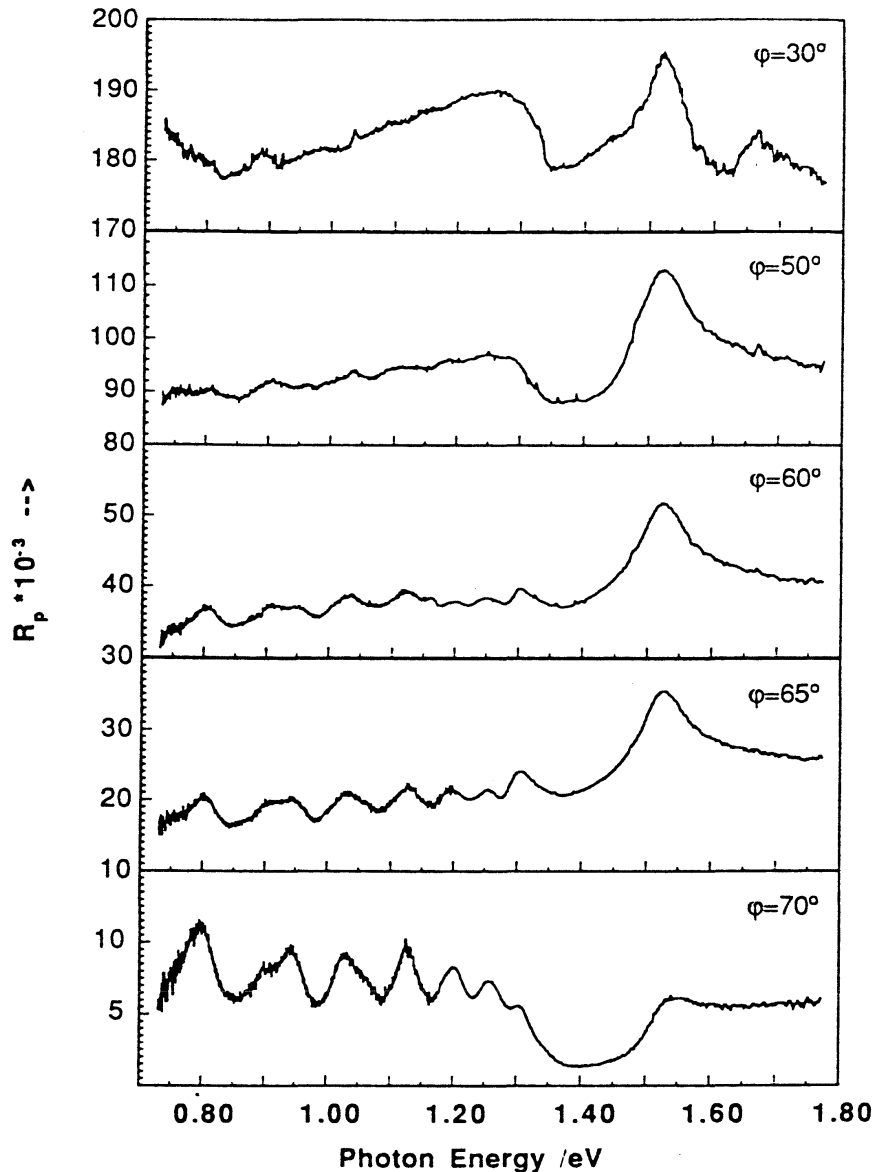


Figure 3: The measured Reflectivity R_p for various angles of incidence ($\varphi=30^\circ$, $\varphi=50^\circ$, $\varphi=60^\circ$, $\varphi=70^\circ$;) shows the advantages of the method. The Reflectivity close to the Brewster angle, φ_B , ($\varphi=70^\circ$) clearly shows absorption centers.

With angles closer to the Brewster angle φ_B ($\varphi=50^\circ$, $\varphi=60^\circ$ and $\varphi=65^\circ$) several

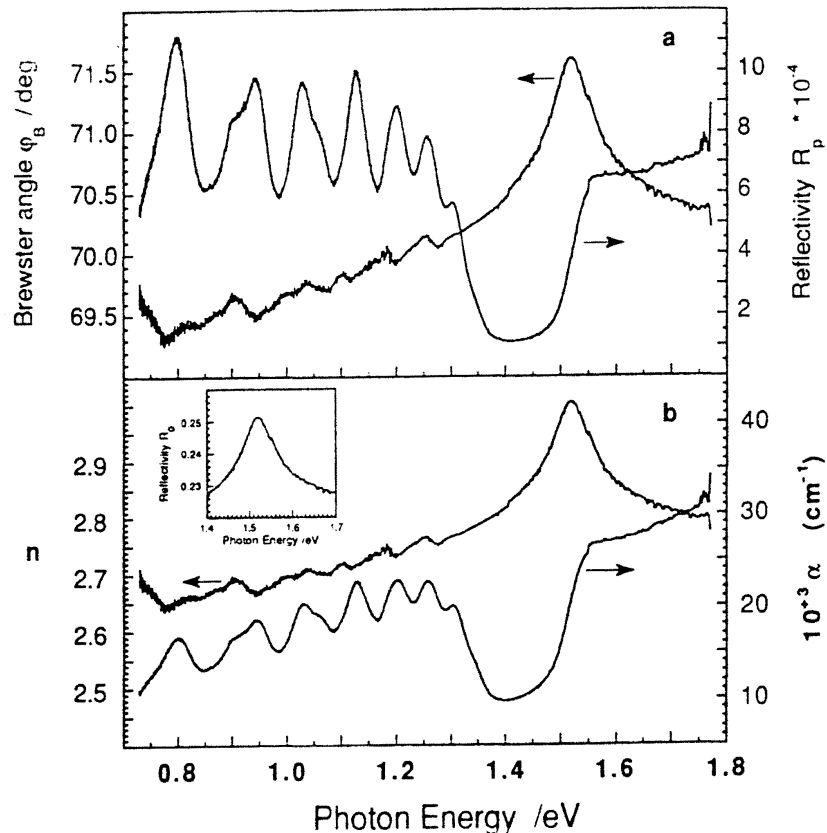
structures can be observed. With an angle $\varphi=70^\circ$ close to the Brewster angle, the formation of defect structures are clearly visible. The reflectivity decreases from about 20% at $\varphi=30^\circ$ to values smaller than 1% at $\varphi=70^\circ$. At the Brewster angle reflectivity smaller than 10^{-4} is detected. The accuracy of the measured reflectivity is in the 10^{-5} - 10^{-6} range since the method is a type of nulling experiment.

The spectral dependence of the Brewster angle and the reflectivity at room temperature is shown in Fig. 4a for intrinsic as-grown CuInS₂ (Type A) in the energy range 0.7eV up to 1.8 eV. Fig. 4b shows the calculated refractive index, n , and the absorption coefficient α .

Figure 4

a) The measured spectral dependence of the Brewster angle φ_B and the reflectivity, R_p , at φ_B for intrinsic as-grown CuInS₂. (Type A)

b) Calculated refractive index n and the absorption coefficient α . The insert shows the calculated Reflectivity at normal incidence R_0 with high accuracy for the band gap region.

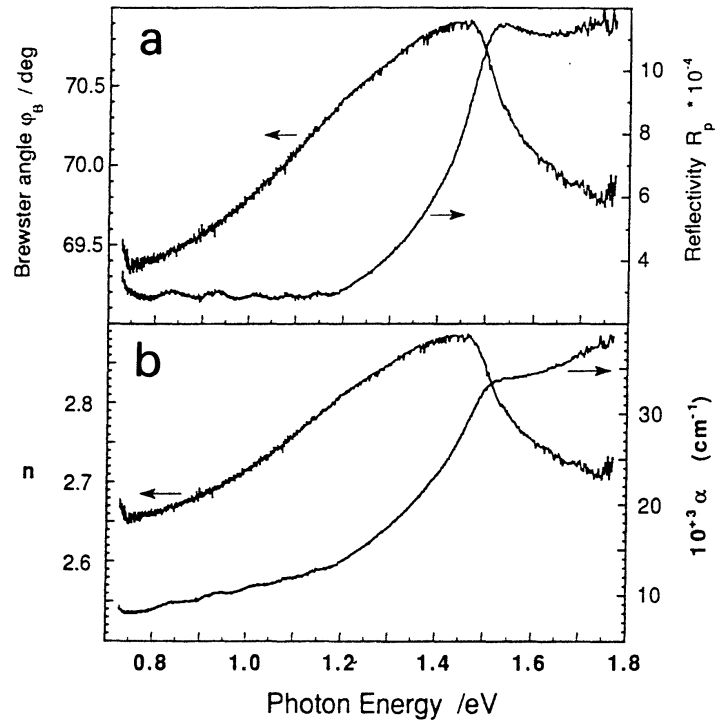


The insert in Fig. 4b displays the calculated reflectivity at normal incidence. A direct band gap transition at 1.556 eV was found. Below the bandgap well pronounced deep level centers at 1.30, 1.256, 1.202, 1.127, 1.032, 0.942 and 0.797 eV were revealed.

The variation of the Brewster angle and reflectivity for a p-CuInS₂ sample (Type B), which is highly self-compensated, is shown in fig. 5.a. The energetic position of the band gap decrease to 1.52 eV with a flatter band tail than shown in Fig 4b. The variation of the bandgap with the carrier concentration was investigated for differently doped n- and p-type GaAs samples[31]. For highly p-doped material the band gap decreases and the absorption within the bandtail increases. The broad structure in the refractive index, n , below the band gap indicates a high concentration of dislocations but these dislocations do not result in a high absorption. Below the band tail, absorption centers at 1.146, 1.088, 1.03, 0.94 and 0.84 eV were observed.

Figure 5a) The spectral dependence of the Brewster angle φ_B and the reflectivity R_p at φ_B for CuInS_2 (Type B). Here a broad structure below the band gap (at 1.52 eV) in the refractive index n indicates a high concentration of dislocations.

b) Calculated refractive index n and the absorption coefficient α .



The transmission spectra of both types of CuInS_2 are shown in Fig. 6. Only a broad absorption structure at about 1.40 eV is detectable. The transmissions below

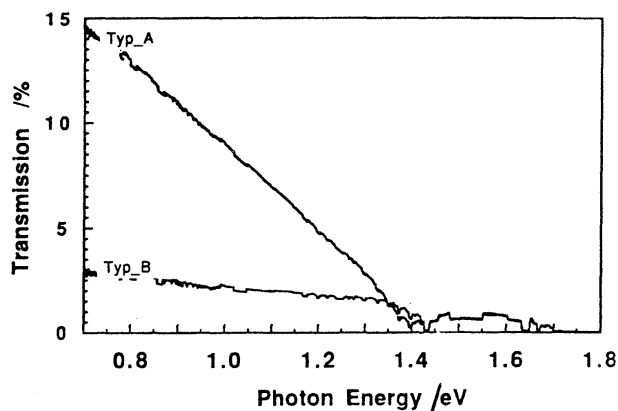


Figure 6: Transmission spectra for CuInS_2 (Type A, Type B) at room temperature

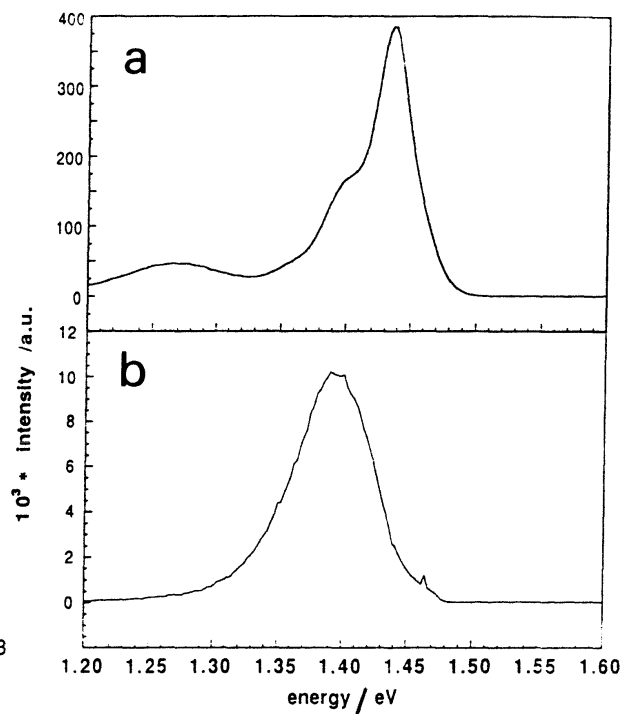


Figure 7: Photoluminescence spectra at 5 K for Type A (a) and Type B (b) CuInS_2 crystals.

1.4 eV are associated with the different sample thicknesses. The results are not helpful in identifying the defect level in the CuInS₂ materials.

In Fig. 7 the photoluminescence (PL) spectra of the two different types of CuInS₂ material are shown. The intrinsic single crystal CuInS₂ (Type A) in fig. 7a shows two emission peaks at 1.435 and 1.40 eV, which lies about 20 meV lower than earlier reported for In-rich CuInS₂[3, 4]. This sample shows a similar behaviour like the lamellar-type of CuInS₂, shown in Fig. 6,b. (part 1). It shows, however, an added broad emission at about 1.27 eV, which is associated with a sulfur excess[32]. The PL spectra of CuInS₂ (Type B) in Fig. 7b show only one broad emission structure at 1.39 eV, which is correlated to a Cu-excess[4]. The broad low energetic emission, shown in Fig. 6a (part 1), which can be attributed to sulphur excess, is missing here.

4. CONCLUSIONS

It has been shown that the Brewster angle spectroscopy method provides a powerful tool in investigating deep levels as well as the optical constants of semiconductors. The deep defect levels found by the BAS-method provide additional information to the information obtained by photoluminescence. Both methods, Photoluminescence and Brewster angle spectroscopy, are complimentary to the identification of the defect-chemistry of CuInS₂.

5. REFERENCES

- 1 B. Tell, J.L. Shay and H.M. Kasper, Phys. Rev. B **4** (1971) 2463.
- 2 G. Massé, N. Lahlou and C. Butti, J. Phys. Chem. Solids **42** (1981) 449-454.
- 3 J.J.M. Binsma, L.J. Giling and J. Bloem, J. Lumin. **27** (1982) 55 - 72.
- 4 J.J.M. Binsma, L.J. Giling and J. Bloem, J. Lumin. **27** (1982) 35 - 53.
- 5 P. Lange, H. Neff, M.L. Fearheiley and K.J. Bachmann, J. Electronic Mat. **14** (1985) 667-76.
- 6 H.J. Hsu, M.H. Yang, R.S. Tang, T.M. Hsu and H.L. Hwang, Journal of Crystal Growth **70** (1984) 427 - 432.
- 7 B. Abid, J.R. Gong, H.G. Goslowsky and K.J. Bachmann, IEEE (1987) 1305
- 8 T.M. Hsu, S.F. Fan and H.L. Hwang, Phys.Lett. **99A** (1983) 255.
- 9 H. Neff, P. Lange, M.L. Fearheiley and K.J. Bachmann, Appl. Phys. Lett. **47** (1985) 1089-1091.
- 10 T.M. Hsu, J.S. Lee and H.L. Hwang, J. Appl. Phys. **68** (1990) 283-187.
- 11 B. Tell, J.L. Shay and H.M. Kasper, J.Appl.Phys. **43** (1972) 2469.
- 12 L.Y. Sun, L.L. Kazmerski, A.H. Clark, P.J. Ireland and D.W. Morton, J. Vac. Sci. Technol. **15** (1978) 265-8.
- 13 R.M.A. Azzam and N.M. Bashara *Ellipsometry and polarized light.*; North-Holland Physics Publishing, Amsterdam; The Netherlands (1987).
- 14 H.B. Holl, J. Opt. Soc. Am. **57** (1967) 683.
- 15 H.J. Lewerenz and N. Dietz, Appl. Phys. Lett. **submitted** (1991)
- 16 N. Dietz and H.J. Lewerenz, Phys. Rev. Lett. **submitted** (1991)
- 17 R. Haak and D. Tench, J. Electrochem. Soc. **131** (1984) 275-283.
- 18 J.C. Bourgoin and H.J.v. Bardeleben, J. Appl. Phys. **64** (1988) R65 - R91.
- 19 M.O. Manasreh, W.C. Mitchel and D.W. Fischer, Appl. Phys. Lett. **55**(1989) 864.
- 20 J.-i. Nishizawa, Y. Oyama and K. Dezaki, J. Appl. Phys. **67** (1990) 1884-1896.

- 21 D.T.F. Marple, *J. Appl. Phys.* **35** (1964) 1241.
- 22 D.E. Aspnes and A.A. Studna, *Phys. Rev. B* **27** (1983) 985-1009.
- 23 A. Sadao, *J. Appl. Phys.* **66** (1989) 6030-6040.
- 24 M.D. Sturge, *Phys. Rev.* **127** (1962) 768.
- 25 D.D. Sell and H.C. Casey, *J. Appl. Phys.* **45** (1974) 800.
- 26 H.C. Casey, D.D. Sell and K.W. Wecht, *J. Appl. Phys.* **46** (1975) 250.
- 27 M.L. Fearheiley and K.J. Bachmann. Symposium on Materials and New Processing Technologies for Photovoltaics; Electrochemical Society Meeting in San Francisco, edited by J. A. Amick, V. J. Kapur and J. Dietl, , 469 (1983).
- 28 M.L. Fearheiley, N. Dietz and H.J. Lewerenz, *J. Electrochem. Soc.* **submitted** (1991)
- 29 N. Dietz and H.J. Lewerenz, in preparation (1991)
- 30 A.W. Verheijen, L.J. Giling and J. Bloem, *Mater. Res. Bull.* **14** (1979) 237.
- 31 Casey, H. C. Sell, D. D. Wecht, *J. Appl. Phys.* **46** (1975) 250--257
- 32 H. Goslowsky, S. Fiechter, R. Könenkamp and H.J. Lewerenz, *Sol. Energy Mater.* **13** (1986) 221.